Engineering Journal issn: 0125-8281

Article

Effect of Labral Tear, Repair and Reconstruction on Strain Distribution in Hip Joint

Panya Aroonjarattham[1,a], Nadhaporn Saengpetch[2,b], Chanatkarn Angsutanasombat[3,c], Chompunut Somtua[1,d], and Kitti Aroonjarattham[4,e,*]

1 Department of Mechanical Engineering, Faculty of Engineering, Mahidol University, Nakornpathom 73170, Thailand
2 Department of Orthopaedics, Faculty of Ramathibodi Hospital, Mahidol University, Bangkok 10400, Thailand
3 Magnecomp Precision Technology PCL, Ayutthaya 13170, Thailand
4 Department of Orthopaedics, Faculty of Medicine, Burapha University, Chonburi 20131, Thailand
E-mail: [a]panya.aro@mahidol.ac.th, [b]doctorobb@gmail.com, [c]ghing009@gmail.com, [d]chompunut.somtua@gmail.com, [e,*]kittaroon@gmail.com (Corresponding author)

Abstract. Labral tear can be caused by degeneration or traumatic hip dislocation. It can be treated by mainly two surgical options: labral repair and labral reconstruction by using tissue reconstruction (iliotibial band), depending on the tear size. Finite element analysis was, thus used to simulate strain distribution in different conditions, namely intact labrum, labral tear, labral repair and labral reconstruction, varied under walking and stair-climbing conditions. By applying labral repair, the labrum thickness was reduced, resulted in increased the average maximum strain on labrum tissue by 21.36% compared to torn labrum, while labral reconstruction reduced the average maximum strain through load sharing of iliotibial band by 28.49% compared to torn labrum and 41.21 % compared to labral repair. The equivalent of total strain of the varied cases did not exceed 25,000 microstrain, not causing bone fracture. The hip model was validated by measuring the normal contact force at the hip joint of a cadaver using hip simulation machine and compared with the simulation result. The simulation result corresponded to the validation test.

Keywords: Labral tear, hip joint, acetabular labrum, labral tissue.

ENGINEERING JOURNAL Volume 25 Issue 6
Received 9 December 2020
Accepted 5 June 2021
Published 30 June 2021
Online at https://engj.org/
DOI:10.4186/ej.2021.25.6.97

DOI:10.4186/ej.2021.25.6.97

1. Introduction

Hip joint is a ball and socket joint that connected femur and pelvis that had a fibrocartilaginous structure layering over the acetabular rim on the non-articular side, called labrum. The labrum covered most of the acetabulum except inferior area that had acetabular ligament. Blood supply of labrum came from vessels around the capsule joint. Labral nerves were from the branch of obturator nerves and quadratus femoris nerves [1]. Free nerve endings found in the labrum were the pain receptors when the labrum was injured [2].

Acetabular labrum is a connective tissue between femoral head and acetabulum that transmits load, connects and stabilizes a joint, disperses pressure of articular surface and seals the fluid inside a hip joint [3, 4, 5, 6, 7]. Labral tear can occur as a result of an excessive movement such as a twisted leg or a hip dislocation and can be treated by surgeries. The two main surgical treatments were labral repair, which was a method of suture and tying labral tissue to the native tissue, and labral reconstruction, which was a tissue replacement of the iliotibial band, filling the missing part of labrum as shown in Fig. 1(a) and 1(b) respectively [8, 9].

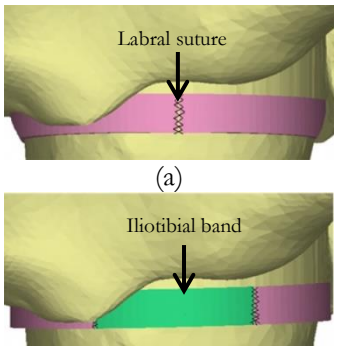

Fig. 1. Surgical treatments: (a) Labral repair and (b) Labral reconstruction.

This research aimed to evaluate the strain distribution on the bone under four labral conditions: intact labrum, radial-torn labrum, repaired labrum and reconstructed labrum using finite element analysis. The result could provide more information, in addition to age, underlying disease, degeneration of joint, type of labral tear that helped surgeon decide on the suitable surgical option.

2. Materials and Methods

2.1. Bone Models

The bone models were simulated by a data from computerized tomography (CT) scanner as shown in Fig. 2(a) and ITK-SNAP program was used to reconstructed three-dimensional bone models by [10, 11, 12, 13] as shown in Fig. 2(b).

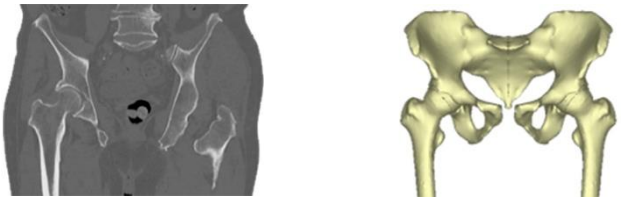

Fig. 2. The bone models: (a) CT slices data and (b) 3D model.

2.2. The Connective Tissue

The connective tissue: acetabular cartilage, femoral cartilage and labrum were simulated by SolidWorks software, fit in the actual anatomical position as shown in Fig. 3.

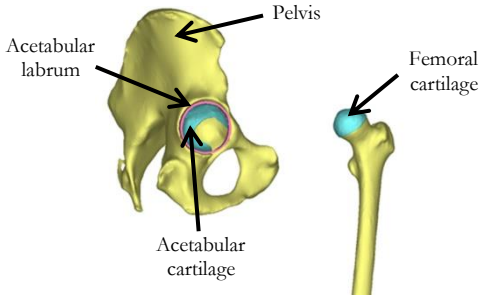

Fig. 3. The position of acetabular labrum, acetabular cartilage and femoral cartilage [14].

Labral tissue was recreated in different conditions: intact labrum, labral tear, labral repair, labral reconstruction with iliotibial band, and hip joint without labrum as shown in Fig. 4.

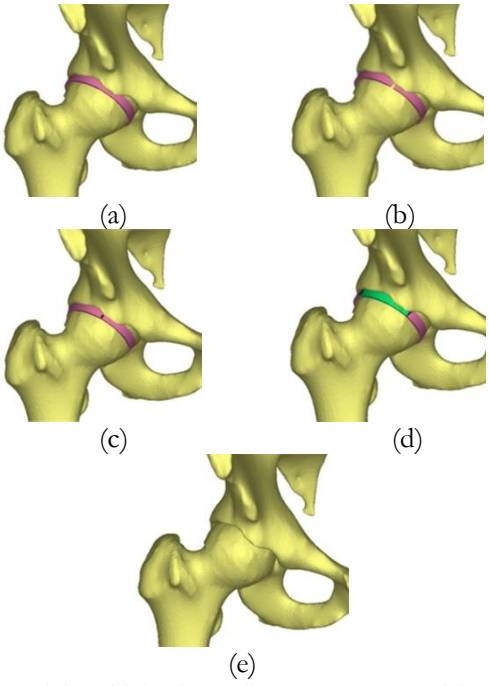

Fig. 4. Models of labral conditions: (a) Intact labrum, (b) Labral tear, (c) Labral repair, (d) Labral reconstruction and (e) Hip joint without labrum.

2.3. Material Properties

Material properties in all parts of the model namely cortical bone, cancellous bone and all connective tissue were assumed as homogeneous, isotropic and linear elastic as shown in Table 1.

Table 1. Material properties of bone and hip joint components [15, 16, 17, 18, 19].

Materials	Elastic Modulus (MPa)	Poisson's Ratio
Cortical bone	17,000	0.290
Cancellous bone	600	0.200
Cartilage	11.63	0.450
Labral tissue	33	0.478
Iliotibial band	111	0.418

2.4. Loading Condition

To compare the effect of labral tissue conditions on strain distribution, the three-dimensional models were analyzed under two loading conditions: walking and stair-climbing. Body weight and muscular forces acted on pelvis and femur [20] as shown in Fig. 5. Table 2 and 3 showed the magnitude of muscular force under walking and stair-climbing conditions respectively.

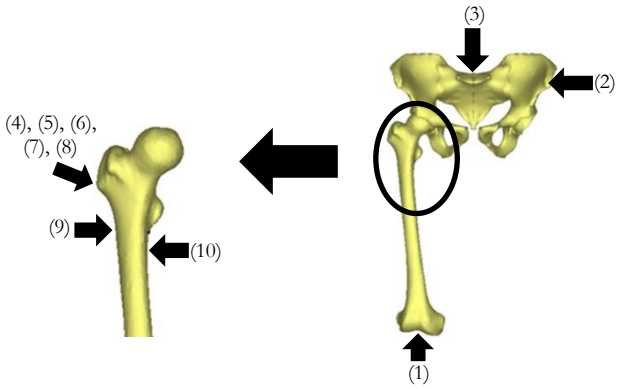

Fig. 5. Loading of force on pelvis and femur.

Table 2. The magnitude of muscular force act on x-, y- and z-axis applied to pelvis and femur under walking condition [20].

Position	Force	Walking Condition		
		F_x (N)	F_y (N)	F_z (N)
(1)	Femoral fix	0	0	0
(2)	Rotational fix	0	0	-
(3)	Body weight	0	0	-836.0
(4)	Abductor	58.0	4.3	86.5
(5)	Ilio-tibial tract, proximal	0	0	0
(6)	Ilio-tibial tract, distal	0	0	0
(7)	Tensor fascia latae, proximal	7.2	11.6	13.2
(8)	Tensor fascia latae, distal	-0.5	-0.7	-19.0
(9)	Vastus lateralis	-0.9	18.5	-92.9
(10)	Vastus medialis	0	0	0

Table 3. The magnitude of muscular force act on x-, y- and z-axis applied to pelvis and femur under stair-climbing condition [20].

Position	Force	Stair-climbing Condition		
		F_x (N)	F_y (N)	F_z (N)
(1)	Femoral fix	0	0	0
(2)	Rotational fix	0	0	-
(3)	Body weight	0	0	-847.0
(4)	Abductor	70.1	28.0	84.9
(5)	Ilio-tibial tract, proximal	10.5	3.0	12.8
(6)	Ilio-tibial tract, distal	-0.5	-0.8	-16.8
(7)	Tensor fascia latae, proximal	3.1	4.9	2.9
(8)	Tensor fascia latae, distal	-0.2	-0.3	-6.5
(9)	Vastus lateralis	-2.2	22.4	-135.1
(10)	Vastus medialis	-8.8	39.6	-267.1

2.5. Cases Analysis

Finite element analysis (FEA) was used to simulate the labral conditions using MSC software package with ten conditions separated by two loading conditions and five labral models as shown in Table 4. Strain distribution on the bone and connective tissue of each case was compared.

Table 4. Case analysis.

Loading Condition	Labral conditions
Walking	Intact labrum
	Labral tear
	Labral repair
	Labral reconstruction
	Hip joint without labrum
Stair-climbing	Intact labrum
	Labral tear
	Labral repair
	Labral reconstruction
	Hip joint without labrum

2.6. Convergence Test and Mesh Generation

A convergence test was used to optimize mesh size in order to reduce calculation time. The four-node tetrahedral elements were used for these models because they can be easily applied to meshing any types and shapes of objects regardless of their complexity. The contact condition between hip and femur model was a touch condition and the rest were of a glue condition. The mesh size of hip joint was varied from 0.175 to 0.2, 0.225, 0.25, 0.275, 0.3 and 0.35 millimeters. Mesh size of 0.25 was selected because it was the biggest size that represented the steadiness of equivalent of total strain of the smaller ones, generating 111,164 nodes and 455,399 elements as shown in Fig. 6.

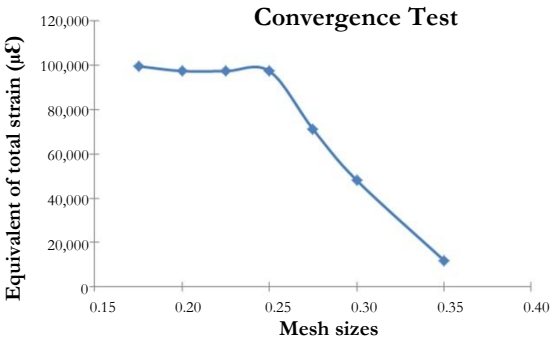

Fig. 6. The relationship between equivalent of total strain on hip joint and mesh sizes.

The total number of nodes and elements of each studied model was show in Table 5 and the mesh model was shown in Fig. 7.

Table 5. Total number of nodes and elements of all labral conditions.

Labral condition	Total number of nodes	Total number of elements
Intact labrum	111,164	455,399
Labral tear	110,668	453,319
Labral repair	109,041	445,579
Labral reconstruction	110,554	452,405
Hip joint without labrum	95,801	394,296

Fig. 7. Mesh model of hip joint.

3. Results and Discussion

Finite element analysis was used to evaluate the strain distribution on the 3D models of five labral conditions under walking and stair-climbing load.

3.1. Labral Models

The maximum and average equivalent of total strain of all models were shown in Table. 6.

Table 6. The maximum and average of equivalent of total strain (με) of all labral models under walking and stair-climbing conditions.

Condition	Walking		Stair-climbing	
	Maximum	Average	Maximum	Average
Intact labrum	70,515	6,470	56,861	5,853
Labral tear	63,825	6,348	63,199	5,966
Labral repair	65,712	7,410	61,242	7,518
Labral reconstruction	54,023	4,089	61,140	4,691

The maximum and average strain distribution of intact labrum was used to compare with the other cases. In case of labral tear, the tear did not affect the average strain under both conditions but the concentrated strain occurred around the tear. In case of labral repair, repairing the tear reduced the labrum thickness while increases the equivalent of total strain on labrum tissue. In case of labral reconstruction, the strain on labral reconstruction was reduced by load sharing from iliotibial band that had a higher elastic modulus than labrum, resulting lower equivalent of total strain than other conditions.

3.2. Cartilaginous Layer

Cartilaginous layer was a direct contact between acetabular and femoral cartilage. The strain distribution on cartilage for each labral condition was used to analyze and hip joint without labrum was observed. The maximum and average of equivalent of total strain on acetabular and femoral cartilage under walking and stair-climbing conditions was shown in Table 7 and 8 respectively.

Table 7. The maximum and average of equivalent of total strain (με) on acetabular cartilage under walking and stair-climbing conditions.

Condition	Walking		Stair-climbing	
	Maximum	Average	Maximum	Average
Intact labrum	210,488	21,684	236,150	22,372
Labral tear	204,070	22,384	250,984	23,080
Labral repair	217,475	22,757	236,695	23,422
Labral reconstruction	202,991	22,152	241,031	23,139
Hip joint without labrum	237,254	25,263	251,963	25,645

Table 8. The maximum and average of equivalent of total strain (με) on femoral cartilage under walking and stair-climbing conditions.

Condition	Walking		Stair-climbing	
	Maximum	Average	Maximum	Average
Intact labrum	145,855	11,945	154,101	11,605
Labral tear	149,606	12,126	158,742	11,783
Labral repair	147,143	11,587	156,351	11,886
Labral reconstruction	147,248	11,519	150,544	12,263
Hip joint without labrum	166,087	11,122	178,518	11,299

The result from each cartilaginous layer showed similar trends of equivalent of total strain while tear labrum showed concentrated strain on some of cartilaginous area. The repair cases showed higher strain on acetabular cartilage than other cases while the model without labrum showed the highest strain on the cartilaginous layer. The equivalent of total strain distribution on femoral cartilage of five models under walking and stair-climbing conditions was shown in Fig. 8 and 9 respectively.

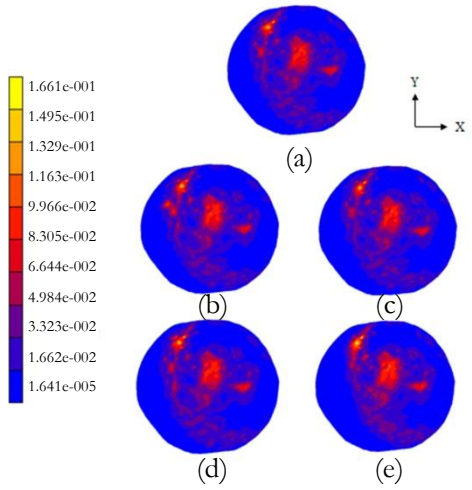

Fig. 8. Equivalent of total strain distribution on femoral cartilage under walking condition: (a) Intact labrum, (b) Labral tear, (c) Labral repair, (d) Labral reconstruction and (e) Hip joint without labrum.

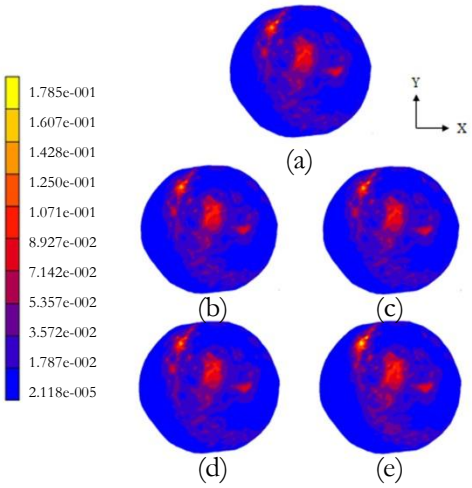

Fig. 9. Equivalent of total strain distribution on femoral cartilage under stair-climbing condition: (a) Intact labrum, (b) Labral tear, (c) Labral repair, (d) Labral reconstruction and (e) Hip joint without labrum.

3.3. Bone Models

The load occurred on the models attached with labral tissue did not affect the equivalent of total strain on the bone while the strain on the hip joint without labrum increased insignificantly as shown in Table 9 and all models provided similar value of the strain on the pelvis, showing maximum of equivalent of total strain at 2,013 and 2,043 microstrain under walking and stair-climbing respectively.

Table 9. The maximum and average of equivalent of total strain (με) on femur under walking and stair-climbing conditions.

Condition	Walking		Stair-climbing	
	Maximum	Mean	Maximum	Mean
Intact labrum	562.00	119.03	777.70	139.21
Labral tear	562.01	118.80	778.40	139.00
Labral repair	563.94	119.62	777.50	139.03
Labral reconstruction	564.64	119.40	777.01	138.53
Hip joint without labrum	565.58	121.18	779.58	140.36

The equivalent of total strain distribution on five femoral models was shown in Fig. 10 and 11 under walking and stair-climbing conditions respectively.

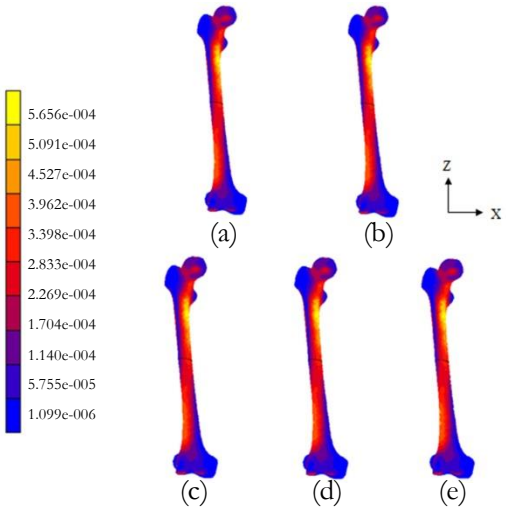

Fig. 10. Equivalent of total strain distribution on five femoral models under walking condition: (a) Intact Labrum, (b) Labral Tear, (c) Labral Repair, (d) Labral Reconstruction and (e) Hip joint without labrum.

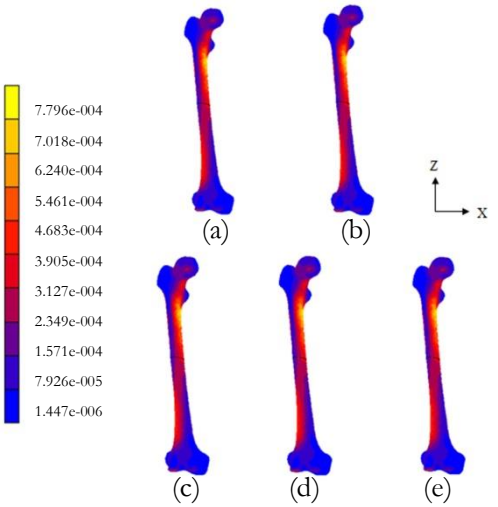

Fig. 11. Equivalent of total strain distribution on five femoral models under stair-climbing condition: (a) Intact Labrum, (b) Labral Tear, (c) Labral Repair, (d) Labral Reconstruction and (e) Hip joint without labrum.

3.4. Comparison between Labral Conditions

Intact labrum was a natural condition, providing an appropriate equivalent of total strain for hip joint. Each model under the studied conditions was compared to intact condition as shown in Table. 10.

Table 10. The average percentage of equivalent of total strain compared to intact labrum.

Condition	Walking		Stair-climbing	
	Labrum	Cartilage*	Labrum	Cartilage*
Intact labrum	100.00	100.00	100.00	100.00
Labral tear	98.11	102.61	101.95	102.61
Labral repair	114.52	102.13	128.46	103.92
Labral reconstruction	63.19	100.13	80.15	104.20
Hip joint without labrum	-	108.20	-	108.73

*Average value from acetabular and femoral cartilage

To compare the average percentage equivalent of total strain on labrum of all cases with intact labrum: labral tear increased by 0.36%, labral repair showed an increase of 21.49%, labral reconstruction showed a decrease of strain by 28.33% because load transferred was shared to iliotibial band which had more flexibility property. All cases with labral tissue did not affect the cartilaginous layer. Removal of labrum slightly increased the average of equivalent of total strain on cartilaginous layer. The bone model of all cases had the equivalent of total strain less than 25,000 microstrain, meaning that the bone could not fracture [21, 22].

3.5. Validation Test

Research evidence proved the reliability of a bone model created from computerized tomography (CT) scan data [23, 24]. To evaluate the reliability of finite element simulated models, their results needed to be compared to that of the validation test – in this research, the contact normal force. The hip simulation machine [14] was used with a specimen selected by its similar dimensions to that of the finite element model; its contact force was measured by I-Scan sensor (Tekscan Inc., USA). It was installed between acetabular and femoral cartilage inside the hip joint. The cadaveric hip was pressed by 350 N axial loads by Panasonic AC servo motor and a pelvis locker was installed to prevent specimen rotation as shown in Fig. 12.

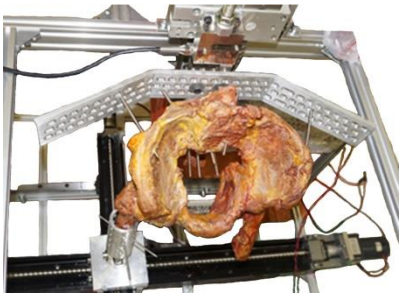

Fig. 12. The hip simulation machine.

The constant load was set by ZEGA S-type KEED-100KG load cell. The cadaveric labrum was tested in three labral conditions: intact labrum - a natural labral tissue without any dissection, labral repair – torn labrum dissected and sutured, and labral reconstruction – labrum where the tissue at anterior-superior region was removed and replaced by iliotibial band. The cadaver showed the averaged contact normal force of 279.48±27.53 N for intact labrum, 294.84±40.81 N for labral repair and 144.72±108.31 N for labral reconstruction.

The boundary condition was reset to match that of the validation testing - pelvis was compressed by 350 N of axial load while preventing rotation. The contact normal force between acetabular and femoral cartilage including intact labrum, labral repair and labral reconstruction were 347.71 N, 351.77 N and 342.17 N respectively. The discrepancy between simulation and validation testing was 19.62%, 16.18% and 57.71% respectively as show in Fig. 13.

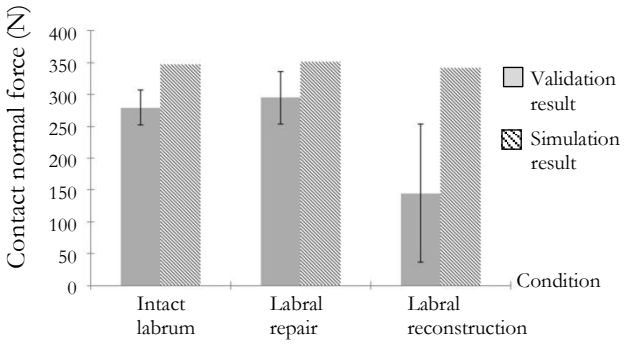

Fig. 13. The comparison of contact normal force between validation and simulation result.

The contact normal force from validation test was lower than simulation test in all cases because the lateral side of hip without femur as shown in Fig. 5 was not ideally rotational-fixed, resulting in the clockwise moment on the cadaver model.

Intact labrum showed value of contact normal force higher than 20% because the synovial fluid in hip socket shared the load transfer in validation model while the synovial fluid of the simulation model was absent.

Labral repair was a labral tissue dissection of torn labrum. Being torn, the fluid flowed out the socket, making the condition very similar to that of the finite element model, yielding lowest different contact normal force between two results.

Labral reconstruction had the highest different values of contact normal force between validation and simulation model because the properties of iliotibial band were uncontrollable. Several research articles showed that good results still came with discrepancy [23, 25, 26]. The fresh, frozen or embalmed cadaver affects the material properties of illiotibial band. Resulting in different results from mechanical testing [27]. However, the results from the simulation showed that the labral repair and labral reconstruction did not affect the hip contact force.

Normally, the body weight was transferred through bones, muscles, ligaments and tendons [28]. Hip models from CT data were solely bone models but the cadaveric hip in validation testing still had some of the muscles and ligaments attached.

4. Conclusion

The Labrum contributed to the hip joint stability by increasing the articular surface by 22% and increasing

acetabular volume by 33% [29] and the labrum sealing helped promote the negative pressure effect within the hip joint by encapsulating the joint fluid for good movement and hip joint stability [7]. The lack of labrum and the iliofemoral ligament could increase the anterior translation and external rotation of femoral head [3] and shifting the load bearing surface. Without labrum, 40% acceleration in cartilage degeneration could be seen, and an increase up to 92% in femoroacetabular stress could occur as a result of a shifting of the load-bearing surface. [7].

Finite element analysis was an advantage method to assess complicated conditions and analyze certain values that cannot be indicated without destructive testing, for example, the equivalent of total strain on tissues, which was a complex mechanical value. The validation testing was necessary to confirm the reliability of the result from finite element analysis.

The simulation and validation testing showed the same trend of contact normal force. Labral repair and labral reconstruction treatments did not affect hip joint and hip bone components in overall but the simulation result showed the concentrated strain around labral tear and cartilaginous layer, causing pain in labrum torn patients [30, 31, 32]. Labral reconstruction showed lower equivalent of total strain on labrum tissue than the that of the labral repair. In case the tear occurred on more than one positions, the labral repair would make the labral ring tighter and some of the tear may not be possible to treat by labral repair method. The results could be used as a helping guide for surgeons to make a decision in labral surgery.

Acknowledgement

The author wished to thank Faculty of Medicine, Burapha University, Faculty of Medicine, Ramathibodi Hospital and Faculty of Engineering, Mahidol University for their kind support of the facilities.

References

[1] R. Putz and C. Schrank, "Anatomy of the labrocapsular complex of the hip joint," *Orthopade.*, vol. 27, no. 10, pp. 675–680, 1998.

[2] Y. T. Kim and H. Azuma, "The nerve ending of the acetabular labrum," *Clin Orthop Relat Res.*, vol. 320, pp. 176–181, 1995.

[3] C. A. Myers, B. C. Register, P. Lertwanich, L. Ejnisman, W. W. Pennington, J. E. Giphart, R. F. LaPrade, and M. J. Philippon, "Role of the acetabular labrum and the iliofemoral ligament in hip stability: an in vitro biplane fluoroscopy study," *Am. J. Sports Med.*, vol. 39, no. 1_suppl, pp. 85S–91S, 2011.

[4] M. V. Smith, H. B. Panchal, R. A. Ruberte Thiele, and J. K. Sekiya, "Effect of acetabular labrum tears on hip stability and labral strain in a joint compression model," *Am. J. Sports Med.*, vol. 39, no. 1_suppl, pp. 103S–110S, 2011.

[5] N. Espinosa, D. A. Rothenfluh, M. Beck, R. Ganz, and M. Leunig, "Treatment of femoro-acetabular impingment: Preliminary results of labral refixation," *J. Bone Joint Surg. Am.*, vol. 88, no. 5, pp. 925–935, 2006.

[6] L. A. Farjo, J. M. Glick, and T. G. Sampson, "Hip arthroscopy for acetabular labral tears," *Arthroscopy*, vol. 15, no. 2, pp. 132–137, 1999.

[7] S. J. Ferguson, J. T. Bryant, R. Ganz, and K. Ito, "An in vitro investigation of the acetabular labral seal in hip joint mechanics," *J. Biomech.*, vol. 36, no. 2, pp. 171–178, 2003.

[8] L. L. Greaves, M. K. Gilbart, A. C. Yung, P. Kozlowski, and D. R. Wilson, "Effect of acetabular labral tears, repair and resection on hip cartilage strain: A 7 T MR study" *J. Biomech.*, vol. 43, pp. 858–863, 2010.

[9] D. Woyski and R. Mather, "Surgical treatment of labral tears: debridement, repair, reconstruction," *Curr Rev Musculoskelet Med.*, vol. 12, pp. 291–299, 2019.

[10] P. Aroonjarattham, K. Aroonjarattham, and C. Suvanjumrat, "Effect of mechanical axis on strain distribution after total knee replacement," *J. Kasetsart (Nat. Sci.)*, vol. 48, no. 2, pp. 263–282, 2014.

[11] P. Aroonjarattham, K. Aroonjarattham, and M. Chanasakulniyom, "Biomechanical effect of filled biomaterials on distal Thai femur by finite element analysis. *J. Kasetsart (Nat. Sci.)*, vol. 49, no. 2, pp. 263–276, 2015.

[12] K. Chalernphon, P. Aroonjarattham, K. Aroonjarattham, and C. Somtua, "The effect of static and dynamic loading on femoral bone using finite element analysis," *J. Res. Appl. Mech. Eng.*, vol. 6, no. 2, pp. 113–130, 2018.

[13] C. Somtua, P. Aroonjarattham, and K. Aroonjarattham, "The correction of Thai varus knee by high tibial osteotomy with Fujisawa's point using finite element analysis," *J. Res. Appl. Mech. Eng.*, vol. 7, no. 1, pp. 45–59, 2019.

[14] C. Angsutanasombat, N. Saengpetch, P. Nirunsuk, P. Aroonjarattham, K. Aroonjarattham, and C. Somtua, "Design of hip simulation machine for hip labrum testing," *Eng J.*, vol. 22, no. 2, pp. 117–130, 2018.

[15] C. R. Henak, B. J. Ellis, M. D. Harris, A. E. Anderson, C. L. Peters, and J. A. Weiss, "Role of the acetabular labrum in load support across the hip joint," *J. Biomech.*, vol. 44, no. 12, pp. 2201–2206, 2011.

[16] A. Perez, A. Mahar, C. Negus, P. Newton, and T. Impelluso, "A computational evaluation of the effect of intramedullary nail material properties on the stabilization of simulated femoral shaft fractures," *Med Eng Phy*, vol. 30, no. 6, pp. 755–760, 2008.

[17] G. E. Kempson, "The mechanical properties of articular cartilage," in *The joints and synovial fluid*, vol. 2, pp. 177–238, 1980.
[18] S. W. Jang, Y. S. Yoo, H. Y. Lee, Y. S. Kim, P. K. Srivastava, and A. V. Nair, "Stress distribution in superior labral complex and rotator cuff during in vivo shoulder motion: A finite element analysis," *Arthroscopy*, vol. 31, no. 11, pp. 2073–2081, 2015.
[19] B. Innocenti, O. F. Bilgen, L. Labey, G. H. van Lenthe, J. Vander Sloten, and F. Catani, "Load sharing and ligament strains in balanced, overstuffed and under stuffed UKA: a validated finite element analysis," *Arthroplasty*, vol. 29, no. 7, pp. 1491–1498, 2014.
[20] M. O. Heller, G. Bergman, J. P. Kassi, L. Claes, N. P. Hass, and G. N. Duda, "Determination of muscle loading at the hip joint for use in pre-clinical testing," *Biomechanics*, vol. 38, pp. 1155–1163, 2004.
[21] F. Taddei, E. Schileo, B. Helgason, L. Cristofolini, and M. Viceconti, "The material mapping strategy influences the accuracy of CT-based finite element models of bones: an evaluation against experimental measurements," *Med Eng Phy*, vol. 29, no. 9, pp. 973–979, 2007.
[22] H. M. Frost, "Wolff's Law and bone's structural adaptations to mechanical usage: an overview for clinicians," *The Angle Orthodontist*, vol. 64, no. 3, pp. 175–188, 1994.
[23] J. H. Keyak, M. G. Fourkas, J. M. Meagher, and H. B. Skinner, "Validation of an automated method of *J. Biomed. Eng.*, vol. 15, 6, pp. 505–509, 1993.
[24] E. Schileo, E. Dall'Ara, F. Taddei, A. Malandrino, T. Schotkamp, M. Baleani, and M. Viceconti, "An accurate estimation of bone density improves the accuracy of subject-specific finite element models," *J. Biomech*, vol. 41, no. 11, pp. 2483–2491, 2008.
[25] H. M. Frost, "A 2003 update of bone physiology and Wolff's Law for clinicians," *The Angle Orthodontist*, vol. 74(1), pp. 3–15, 2004.
[26] J. H. Keyak, J. M. Meagher, H. B. Skinner, and C. D. Mote, "Automated three-dimensional finite element modeling of bone: A new method," *J. Biomed. Eng.*, vol. 12, no. 5, pp. 389–397, 1990.
[27] X. Li, Y. H. An, Y. D. Wu, Y. C. Song, Y. J. Chao, and C. H. Chien, "Microindentation test for assessing the mechanical properties of cartilaginous tissues," *J Biomed Mater Res B Appl Biomater*, vol. 80, no. 1, pp. 25–31, 2007.
[28] L. Zach, L. Kunčická, P. Růžička, and R. Kocich, "Design, analysis and verification of a knee joint oncological prosthesis finite element model," *Comput Biol Med*, vol. 54, pp. 53–60, 2014.
[29] S. J. Ferguson, J. T. Bryant, R. Ganz, and K. Ito, "The acetabular labrum seal: A poroelastic finite element model," *Clin Biomech (Bristol, Avon)*, vol. 15, no. 6, pp. 463–468, 2000.
[30] J. McCarthy, P. Noble, F. V. Aluisio, M. Schuck, J. Wright, and J. Lee, "Anatomy, pathologic features and treatment of acetabular labraltears," *Clin Orthop*, vol. 406, pp. 38–47, 2003.
[31] M. Schmerl, H. Pollard, and W. Hoskins, "Labral injuries of the hip: A review of diagnosis and management," *J Manipulative Physiol Ther*, vol. 28, no. 8, pp. 632.e1–8, 2005.
[32] M. M. Groh and J. Herrera, "A comprehensive review of hip labral tears," *Curr Rev Musculoskelet Med*, vol. 2, pp. 105–117, 2009.

Panya Aroonjarattham was in Bangkok, Thailand in 1976. He received the Bachelor's degree in Mechanical engineering from Mahidol University, Nakorn Pathom, Thailand in 1998. He received the Master's and Doctoral's degrees in Mechanical engineering from Kasetsart University, Bangkok, Thailand, in 2003 and 2009, respectively. He is currently an Assistant Professor at Department of Mechanical Engineering, Mahidol University, Nakorn Pathom, Thailand. His research interests in Biomechanics, Orthopaedic implant design, Finite Element Analysis, and Machine design.

Nadhaporn Saengpetch was in Bangkok, Thailand in 1973. He received the Doctor of Medicine from Ramathibodi Hospital, Mahidol University, Bangkok, Thailand in 1997. He received the Dipolmate, Thai Board of Orthopaedic Surgery from Ramathibodi Hospital, Mahidol University, Thailand in 2003. He is currently an Assistant Professor at Department of Orthopaedics, Faculty of Medicine Ramathibodi Hospital, Mahidol University, Bangkok, Thailand. His research interests in Knee and shoulder reconstructive surgery, Hip arthroscopic surgery and Biomechanics.

Chanatkarn Angsutanasombat was born in Bangkok, Thailand in 1994. She received the first class honor for Bachelor's degree in Mechanical Engineering from Mahidol University, Nakhon Pathom, Thailand, in 2016 and the Master's degree in Mechanical Engineering from Mahidol University, Nakhon Pathom, Thailand, in 2018. She is currently a Senior Engineer Mechanical Design at Magnecomp Precision Technology PCL. Her research interests in Biomechanics, Finite Element Analysis, Robotic and Machine design.

Chompunut Somtua was born in Bangkok, Thailand in 1988. She recieved the Bachelor's and Master's degree in Mechanical Engineering from Mahidol University, Nakhon Pathom, Thailand in 2012 and 2015 respectively. Currently, she is a Ph.D. candidate in Department of Mechanical Engineering, Mahidol University and Lecture at Department of Mechanical Engineering, Thonburi University, Thailand. Her research interests in Biomechanics and Finite Element Analysis.

Kitti Aroonjarattham was in Bangkok, Thailand in 1978. He received the Doctor of Medicine from Ramathibodi Hospital, Mahidol University, Bangkok, Thailand in 2001. He received the Dipolmate, Thai Board of Orthopaedic Surgery from Ramathibodi Hospital, Mahidol University, Thailand in 2008. He is currently an Assistant Professor at Department of Orthopaedics, Faculty of Medicine, Burapha University, Chonburi, Thailand. His research interests in Biomechanics, Orthopaedic implant design, Finite Element Analysis and Spine surgery.